

## **SUPPLEMENTAL FIGURES**

**Supplemental Table 1: Binding constants of ACVR1 mAbs and Fabs to human ACVR1**

ACVR1 mAb Tested	$k_a$ (1/Ms)	$k_d$ (1/s)	$K_D$ (M)	$t^{1/2}$ (min)
mAb 1	1.31E+06	1.59E-03	1.21E-09	7
mAb 2	7.18E+05	1.63E-04	2.27E-10	71
mAb 3	6.77E+05	1.76E-04	2.60E-10	65
Fab 2	5.49E+05	9.36E-05	1.70E-10	123
Fab 3	6.90E+05	1.06E-04	1.54E-10	109
hACVR1 mAb	2.30E+05	1.33E-03	5.80E-09	9

In order to measure the binding constants of ACVR1 mAbs, mAbs were captured with an anti-human Fc antibody immobilized on a CM5 chip. Different concentrations of hACVR1.mmh (REGN3111) were injected over ACVR1 mAbs at 37°C. In order to measure the binding constants of ACVR1 Fabs, hACVR1.mmh was captured with a myc antibody (REGN642) immobilized on a CM5 chip. Different concentrations of ACVR1 Fabs were injected over hACVR1.mmh at 37°C. Binding rate constants and equilibrium dissociation rate constants were calculated by fitting data using 1:1 Langmuir binding model (Scrubber 2.0c). All 3 ACVR1 Fabs bound to monomeric human ACVR1 with binding kinetics similar (< 2.5-fold difference) to their respective mAbs.

**Supplemental Table 2: Binding constants of ACVR1 mAbs and Fabs to mouse ACVR1**

ACVR1 mAb Tested	$k_a$ (1/Ms)	$k_d$ (1/s)	$K_D$ (M)	$t^{1/2}$ (min)
mAb 1	1.34E+06	1.67E-03	1.24E-09	7
mAb 2	7.13E+05	1.61E-04	2.26E-10	72
mAb 3	6.74E+05	1.81E-04	2.68E-10	64
Fab 2	5.45E+05	9.72E-05	1.78E-10	119
Fab 3	6.53E+05	1.05E-04	1.60E-10	110
hACVR1 mAb	ND	ND	ND	ND

In order to measure the binding constants of ACVR1 mAbs, mAbs were captured with an anti-human Fc antibody immobilized on a CM5 chip. Different concentrations of mACVR1.mmh (REGN3407) were injected over ACVR1 mAbs at 37°C. In order to measure the binding constants of ACVR1 Fabs, mACVR1.mmh was captured with a myc antibody (REGN642) immobilized on a CM5 chip. Different concentrations of ACVR1 Fabs were injected over mACVR1.mmh at 37°C. Binding rate constants and equilibrium dissociation rate constants were calculated by fitting data using 1:1 Langmuir binding model (Scrubber 2.0c). All 3 ACVR1 Fabs bound to monomeric mouse ACVR1 with binding kinetics similar (< 2.5-fold difference) to their respective mAbs. hACVR1 mAb didn't bind mACVR1.mmh in the tested concentration range.

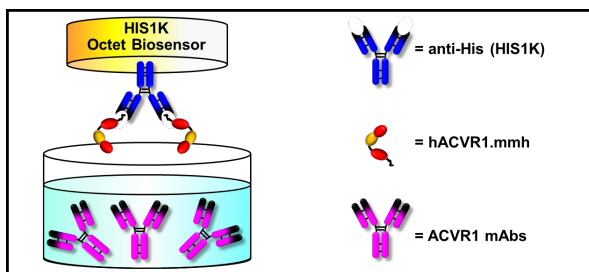
**Supplemental Table 3: ACVR1 antibodies are specific to ACVR1**

mAb Captured	mAb Capture Level (RU)	100 nM Human Receptor Binding				100 nM Mouse Receptor Binding			
		ACVR1	ACVRL1	BMPR1A	BMPR1B	ACVR1	ACVRL1	BMPR1A	BMPR1B
mAb 1	264 ± 4	147 ± 4	2 ± 0	2 ± 0.1	20 ± 0.6	140 ± 2.3	3 ± 0.4	8 ± 0.2	1 ± 0.2
mAb 2	261 ± 0.5	130 ± 0.4	1 ± 0.1	2 ± 0.1	10 ± 0.5	130 ± 1.5	1 ± 0.1	3 ± 0.1	1 ± 0.1
mAb 3	272 ± 2.2	147 ± 2.2	4 ± 0.1	2 ± 0	24 ± 0.6	141 ± 5.4	4 ± 0.4	9 ± 0.1	1 ± 0.1
hACVR1 mAb	251 ± 0.9	98 ± 1.4	0 ± 0.1	0 ± 0.1	3 ± 0.1	63 ± 1.5	0 ± 0.2	1 ± 0.1	0 ± 0.3
Isotype control	236 ± 0.8	11 ± 1.2	2 ± 0	1 ± 0.1	19 ± 0.5	8 ± 1	2 ± 0.2	7 ± 0.1	1 ± 0

In order to measure the specificity of ACVR1 mAbs, ACVR1 mAbs were captured with anti-human Fab immobilized on a CM5 chip. 100 nM or 10 nM of dimeric human or mouse ACVR1, ACVRL1, BMPR1A or BMPR1B were injected at 30  $\mu$ L/min for 2 min (duplicate injections) and the experiment was performed at 25°C. Binding of different receptors to the captured mAb was determined using Scrubber 2.0c. None of the ACVR1 mAbs bound to any of the other receptors indicating that these mAbs are specific to ACVR1.

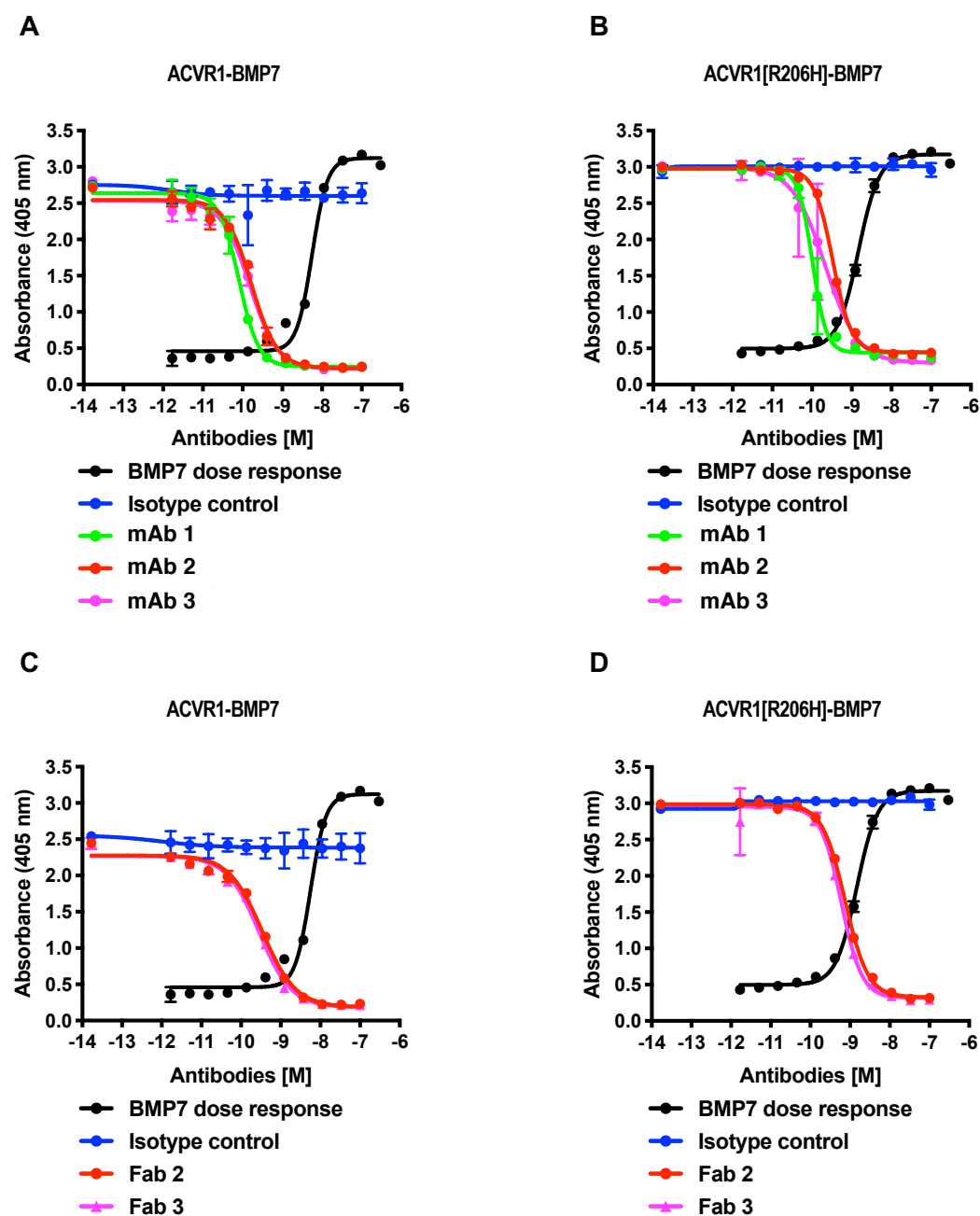
**Supplemental Table 4: Cross-competition data of ACVR1 antibodies**

1 <sup>st</sup> mAb \ 2 <sup>nd</sup> mAb	hACVR1 mAb	mAb 3	mAb 2	mAb 1	Isotype control
hACVR1 mAb	0.04	0.06	0.74	0.80	0.04
mAb 3	0.06	0.03	0.10	0.80	0.05
mAb 2	0.75	0.17	0.04	0.07	0.05
mAb 1	0.75	0.68	0.04	0.04	0.04
Isotype control	0.64	0.65	0.61	0.66	0.07



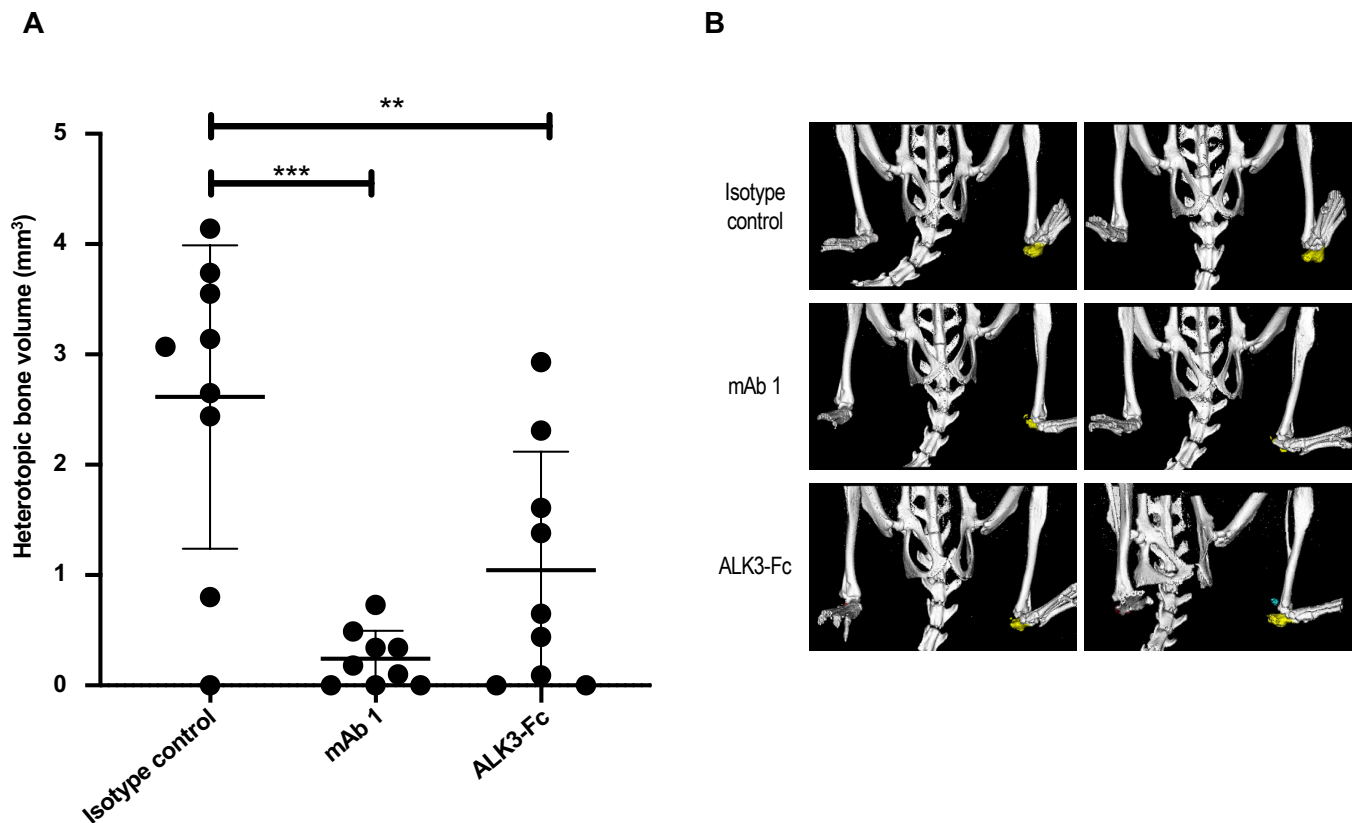
hACVR1.mmh was captured on a His antibody Octet biosensor and was later saturated by dipping into wells containing 50 µg/mL of ACVR1 mAbs (referred to as 1<sup>st</sup> mAb) for 4 min. Then, 1<sup>st</sup> mAb saturated biosensors were dipped into the wells containing 50 µg/mL of different ACVR1 mAbs (referred to as 2<sup>nd</sup> mAb) for 3 min. The binding of 2<sup>nd</sup> mAb to the complex of hACVR1.mmh and 1<sup>st</sup> mAb was determined, and the observed wavelength shift (nm) is reported in the Table. An isotype-matched that doesn't bind ACVR1 was used as a negative control. The cells highlighted in red represent bidirectional competition while white cells represent no competition. A schematic depiction of the experiment is shown below the table.

These data indicate that hACVR1 mAb likely shares an epitope with mAb 3; mAb 3 and mAb2 recognize partially overlapping epitopes (or, alternatively, that binding of one of them to ACVR1 sterically hinders the binding of the other); and that mAb 1 and mAb 2 likely bind overlapping epitopes. Note that there is no cross-competition between hACVR1 mAb and mAb 1 and there is also no cross-competition between mAb 1 and mAb 3, indicating that the epitope recognized by mAb 1 is distinct from that recognized by hACVR1 mAb and mAb 3. Although hACVR1 mAb and mAb 3 appear to recognize overlapping epitopes, their binding properties differ significantly, as hACVR1 recognizes only human ACVR1, whereas mAb 3 recognizes both mouse and human ACVR1 (data not shown). Lastly, there is also no cross-competition between hACVR1 and mAb 2.



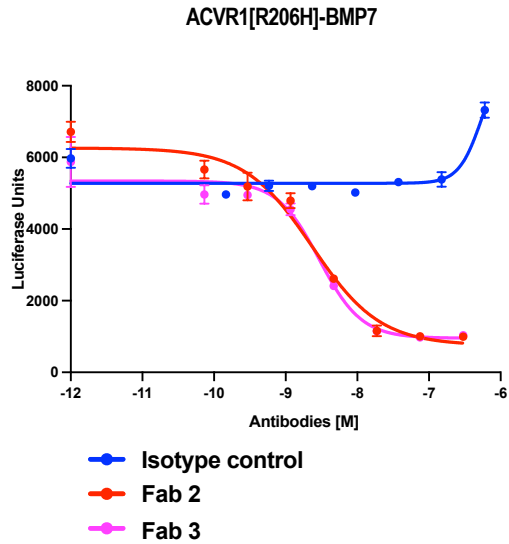
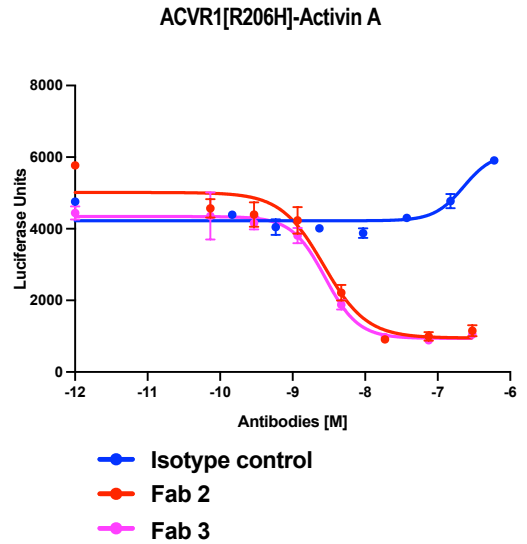
**Supplemental Figure 1: Both ACVR1 antibodies and Fabs block BMP7 induced alkaline phosphatase activity.**

Alkaline phosphatase activity was measured in W20s overexpressing either WT ACVR1 (A, C) or ACVR1[R206H] (B, D). Alkaline phosphatase activity was induced in WT ACVR1 or ACVR1[R206H] overexpressing W20 cells by treating the cells with a fixed concentration (10 nM) of BMP7. Both ACVR1 antibodies and ACVR1 Fabs showed inhibition of alkaline phosphatase activity induced by 10 nM BMP7 in ACVR1 and ACVR1[R206H] overexpressing W20 cells. Data show the mean (n=4) ± SEM. Three biological replicates were performed for the in vitro signaling assays.



**Supplemental Figure 2: ACVR1 antibodies reduce trauma-induced HO (tHO) in WT mice.**

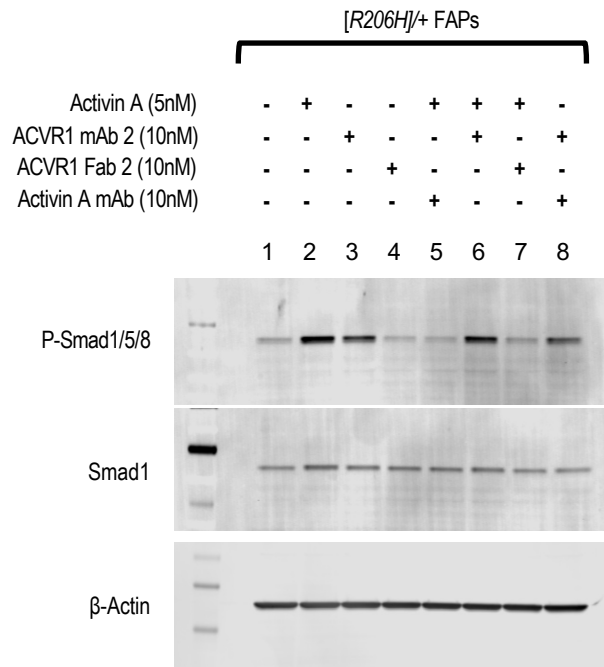
Mice (n=9/group) were administered either isotype control, ACVR1 mAb 1 or ALK3-Fc starting concurrently with induction of injury. Heterotopic bone volume was measured by  $\mu$ CT 5 weeks post injury. ACVR1 mAb 1 and ALK3-Fc significantly reduced heterotopic bone volume compared to isotype control treated mice. Data show the mean  $\pm$  SD, \*\*p<0.01, \*\*\*p<0.001; 1 way ANOVA with Dunnett's multiple-comparison test.

**A****B**

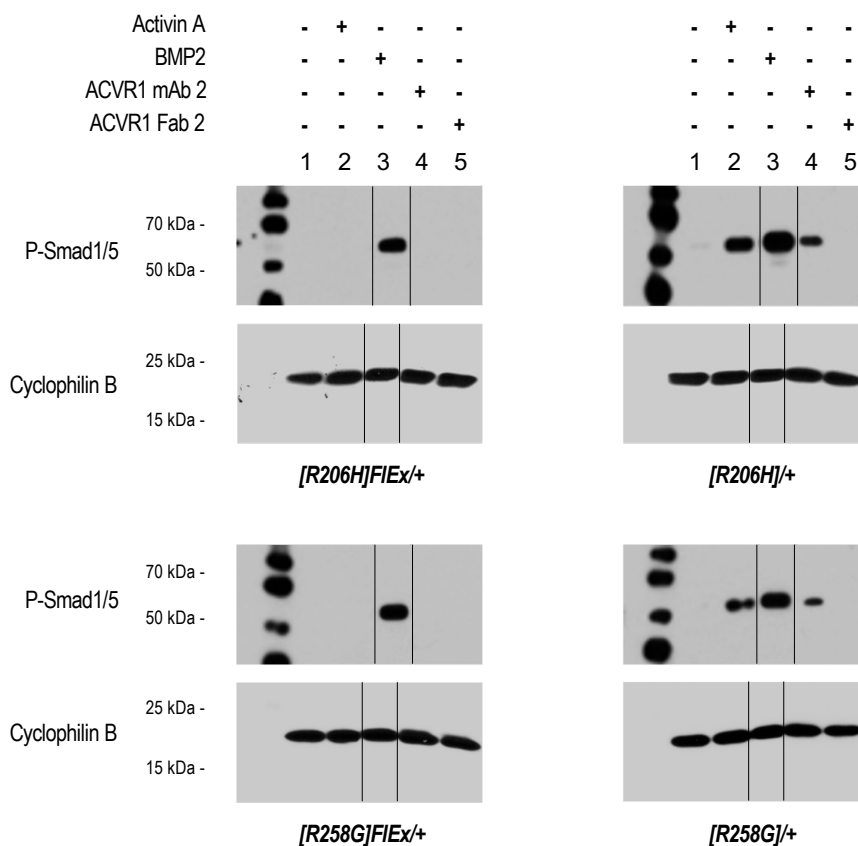
### Supplemental Figure 3: ACVR1 Fabs block BMP7 and Activin A signaling in Hek293.ACVR1[R206H] cells.

Stable pools of Hek293/BRE-Luc reporter cells overexpressing ACVR1[R206H] were treated with a fixed concentration (2 nM) of BMP7 (A) or Activin A (B). ACVR1 Fabs inhibited Smad1/5/8 phosphorylation induced by BMP7 or Activin A. Data show the mean (n=4)  $\pm$  SEM. Three biological replicates were performed for the in vitro signaling assays.



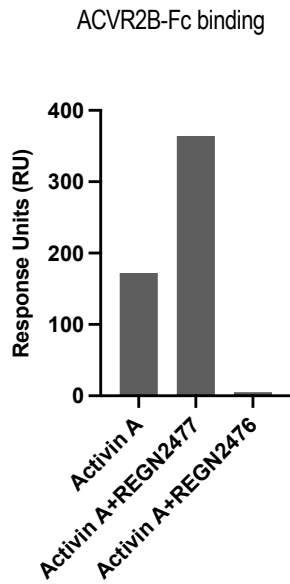
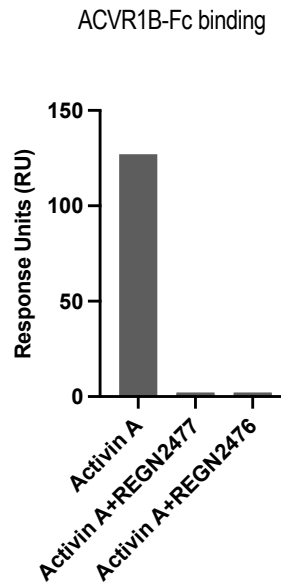


**Supplemental Figure 4: ACVR1 antibodies activate whereas ACVR1 Fabs block ACVR1[R206H].** FAPs isolated from the FOP mice (*Acvr1*<sup>[R206H]<sup>FIE</sup>/+</sup>; *GT(ROSA26)Sor*<sup>CreERT2/+</sup> post tamoxifen) were treated with Activin A, ACVR1 mAb 2, ACVR1 Fab 2 or an Activin A neutralizing mAb (REGN2476) in various combinations for 1 hour. Activin A and ACVR1 mAb 2 but not ACVR1 Fab 2 induced Smad1/5/8 phosphorylation. ACVR1 Fab 2 blocked Activin A induced Smad1/5/8 phosphorylation to background levels, whereas the ACVR1 mAb 2 only partially blocks Activin A induced Smad1/5/8 phosphorylation. The Activin A mAb reduced baseline levels of Smad1/5/8 phosphorylation, and – as would be expected – blocked Activin A induced phosphorylation to background levels.



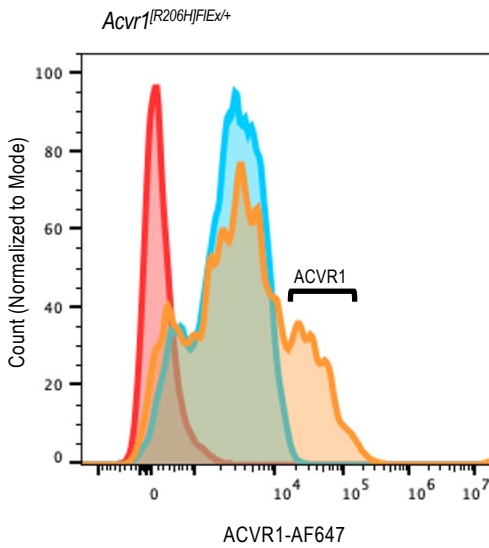
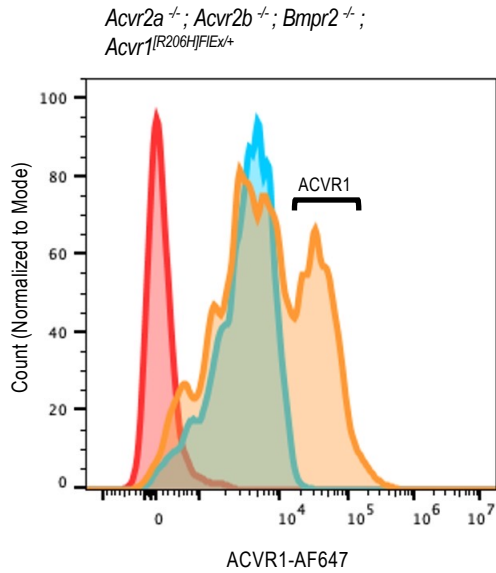
**Supplemental Figure 5: ACVR1 antibodies activate both ACVR1[R206H] and ACVR1[258G], but not wild type ACVR1.**

*Acvr1*<sup>[R206H]FIEx/+</sup>; *GT(ROSA26)Sor<sup>CreERT2/+</sup>* ([R206H]FIEx/+) and *Acvr1*<sup>[R258G]FIEx/+</sup>; *GT(ROSA26)Sor<sup>CreERT2/+</sup>* ([R258G]FIEx/+) mES cells were treated with tamoxifen to generate *Acvr1*<sup>[R206H]/+</sup>; *GT(ROSA26)Sor<sup>CreERT2/+</sup>* ([R206H]/+) and *Acvr1*<sup>[R258G]/+</sup>; *GT(ROSA26)Sor<sup>CreERT2/+</sup>* ([R258G]/+) mES cells. The cells were treated with 10 nM Activin A, BMP2, ACVR1 mAb 2, or ACVR1 Fab 2 in various combinations for 1 hour. Activin A and ACVR1 mAb 2 but not ACVR1 Fab 2 induced Smad1/5/8 phosphorylation both in [R206H]/+ and [R258G]/+ mES cells, but not in [R206H]FIEx/+ and [R258G]FIEx/+ (i.e. wild type) mES cells. BMP2 (used as a positive control) induced Smad1/5/8 phosphorylation in [R206H]FIEx/+, [R258G]FIEx/+, [R206H]/+, and [R258G]/+ mES cells. Thin vertical dividing line indicates that lanes were run on the same gel but were noncontiguous.

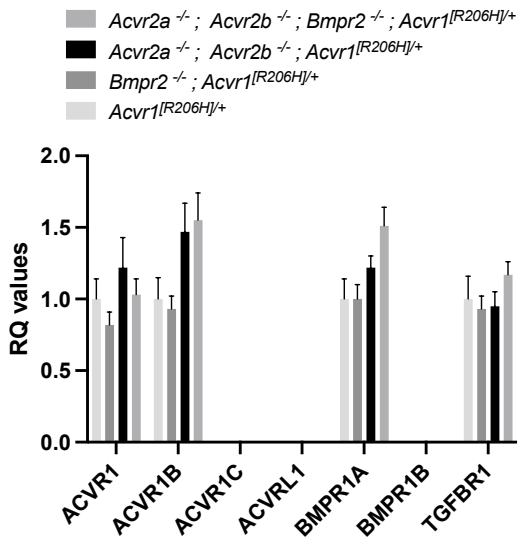
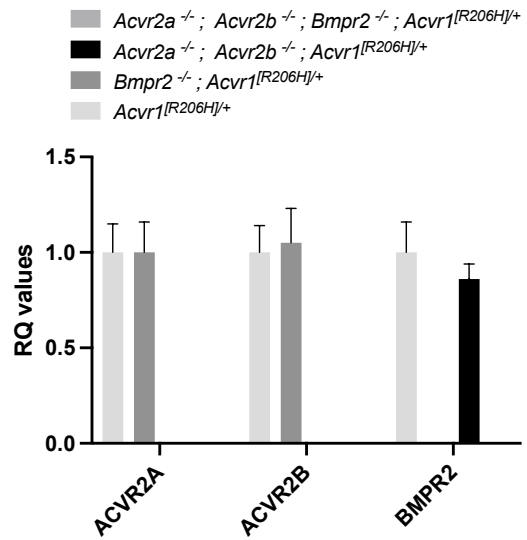
**A****B**

**Supplemental Figure 6: REGN2476 blocks binding of Activin A to both type I and type II receptors, whereas REGN2477 only blocks binding of Activin A to type I receptors.**

ACVR2B-Fc (A) and ACVR1B-Fc (B) were covalently immobilized on a CM5 chip. 5 nM Activin A alone or in complex with REGN2476 and REGN2477 were injected over ACVR2B-Fc and ACVR1B-Fc at 37°C. The association phase response units obtained by Activin A+/-REGN2476/REGN2477 binding to ACVR2B (A) and ACVR1B (B) are displayed in the graph. REGN2476 blocks binding of Activin A to both ACVR1B and ACVR2B, whereas REGN2477 only blocks binding of Activin A to ACVR1B (A-B).

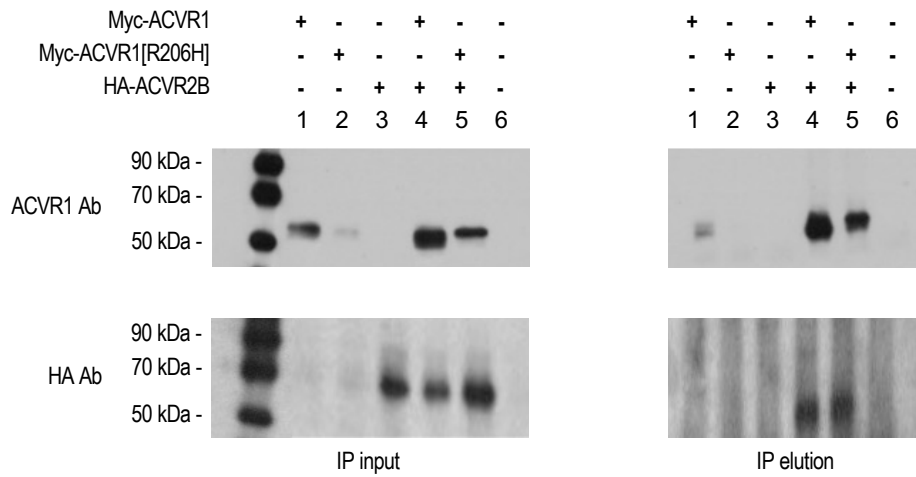
**A****B**

**Supplemental Figure 7: Loss of *Acvr2a*, *Acvr2b* and *Bmpr2* does not affect the expression of ACVR1.** *Acvr1*<sup>[R206H]FIEx+</sup>; *GT(ROSA26)Sor*<sup>CreERT2/+</sup> mES cells (A) and *Acvr1*<sup>[R206H]FIEx+</sup>; *GT(ROSA26)Sor*<sup>CreERT2/+</sup> mES cells lacking *Acvr2a*, *Acvr2b* and *Bmpr2* (B) were stained with an ACVR1 antibody and analyzed by flow cytometry. Both cell lines were positive for ACVR1 expression on the cell surface. Red curves represent unstained cells, blue curves represent only secondary antibody-stained cells, and yellow curves represent ACVR1 primary antibody plus corresponding secondary antibody-stained cells. Hence, ACVR1 is present on the membrane of *Acvr1*<sup>[R206H]FIEx+</sup> mES cells as well as *Acvr1*<sup>[R206H]FIEx+</sup> mES cells lacking *Acvr2a*, *Acvr2b* and *Bmpr2*.

**A****B**

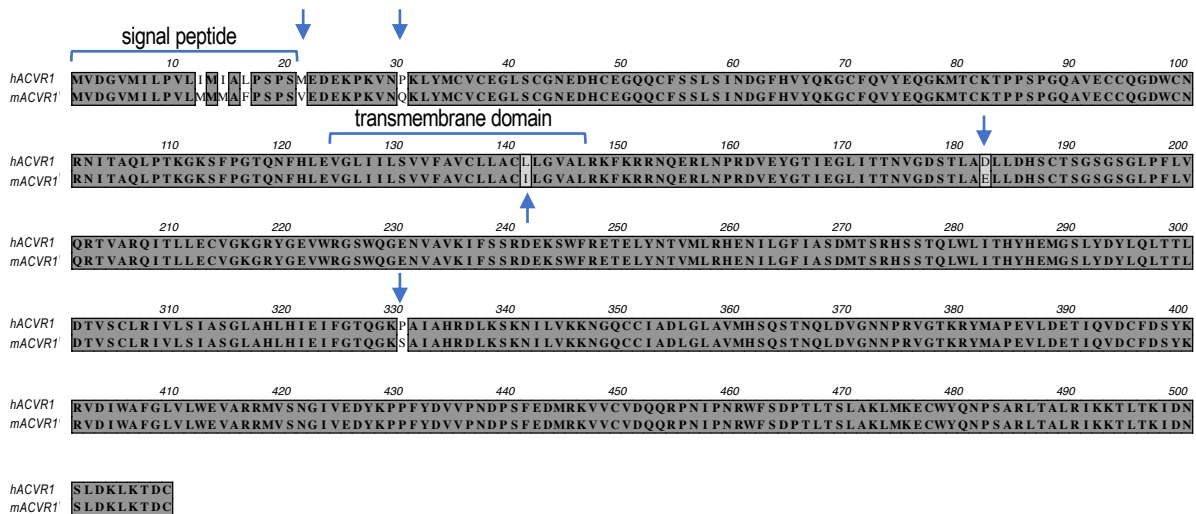
### Supplemental Figure 8: TaqMan analysis of type II receptor KO mES cells.

Type I receptor (A) and type II receptor (B) mRNA levels in *Acvr1*<sup>[R206H]/+</sup>; *GT(ROSA26)Sor<sup>CreERT2</sup>/+* mES cells wherein different combinations of *Acvr2a*, *Acvr2b* or *Bmpr2* have been knocked out. There is no significant difference between type I receptor mRNA levels of different type II receptor KO mES cells (A). Type II receptor mRNA levels remained unchanged in the different lines, except for loss of those type II receptors that have been knocked out (B).



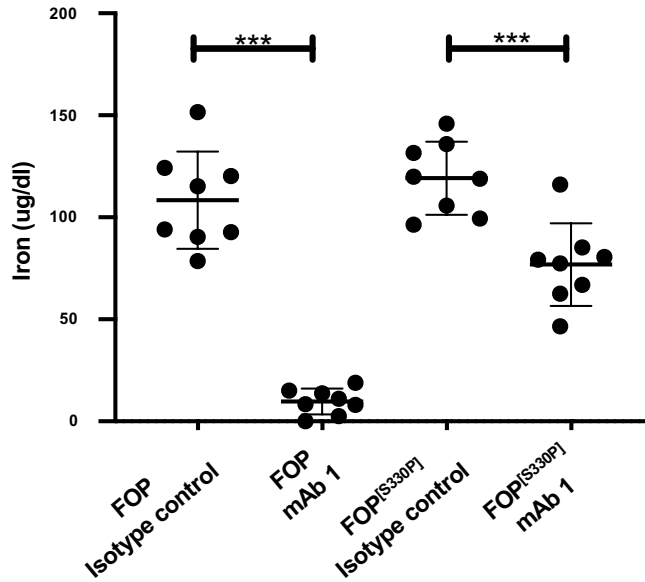
**Supplemental Figure 9: ACVR1 forms heterocomplexes with ACVR2B in the absence of exogenous ligands.**

Hek293 cells were transfected with Myc-tagged ACVR1 and/or HA tagged ACVR2B. ACVR1 was immunoprecipitated using a myc antibody. ACVR1 and ACVR2B were detected using an ACVR1 antibody or HA antibody, respectively. ACVR2B immunoprecipitated with both ACVR1 and ACVR1[R206H] in the absence of exogenous ligands and in the presence of 300 nM ACVR2B-Fc.



**Supplemental Figure 10: Human ACVR1 differs from mouse ACVR1 by two amino acids in the intracellular domain.**

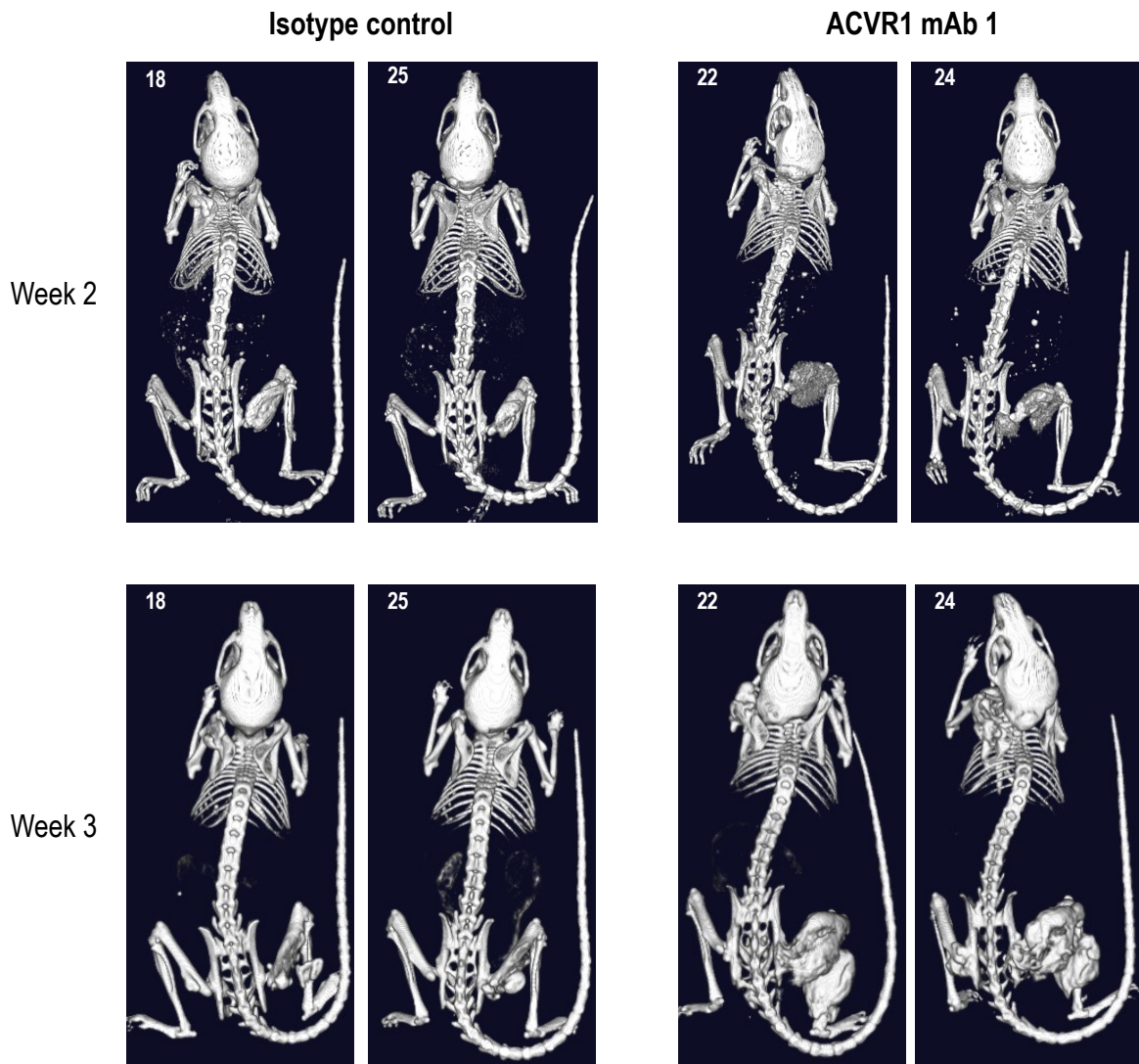
Sequence alignment of human and mouse ACVR1 indicates that they differ by two amino acids in the extracellular domain (amino acids 21 and 30), one amino acid in the transmembrane domain (amino acid 141), and two amino acids in the intracellular domain (amino acids 182 and 330). The corresponding residues are indicated by blue arrows.



**Supplemental Figure 11: ACVR1 mAb 1 reduces serum iron in both FOP and FOP<sup>[S330P]</sup> mice.**

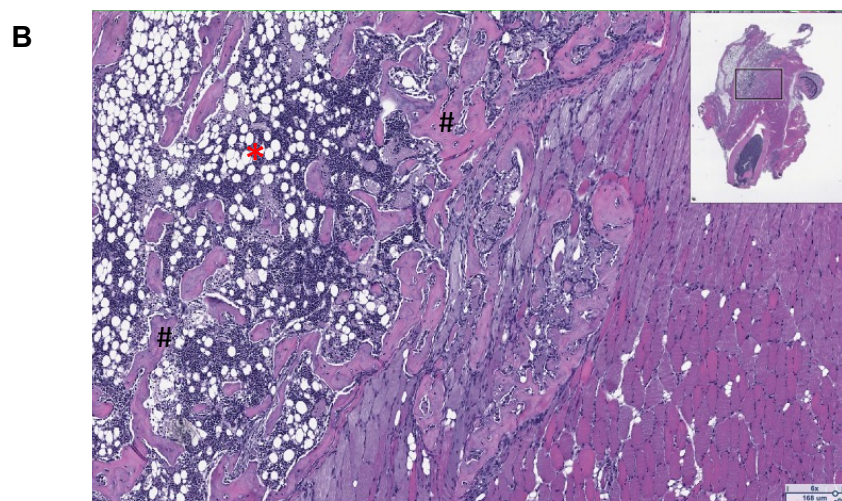
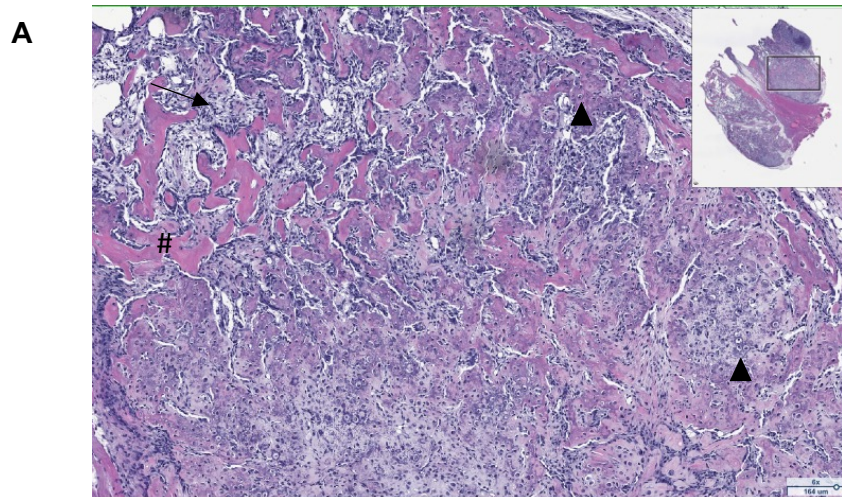
*Acvr1*<sup>[R206H]FIE/+</sup>; *GT(ROSA26)Sor*<sup>CreERT2/+</sup> mice or *Acvr1*<sup>huecto:[R206H]FIE/+;[S330P]</sup>; *GT(ROSA26)Sor*<sup>CreERT2/+</sup> mice were injected with tamoxifen to initiate each model and generate FOP and FOP<sup>[S330P]</sup> mice, respectively. Both mouse lines were concurrently injected with ACVR1 mAb 1 or isotype control antibody at 10 mg/kg weekly. Serum iron was measured at 2 weeks post initiation. ACVR1 mAb 1 decreased serum iron compared to isotype control in both mouse models but to a lesser degree in FOP<sup>[S330P]</sup> mice. N= 8/group, data show the mean  $\pm$  SD, \*\*\* p<0.001 1 way ANOVA with Bonferroni's multiple-comparison test.





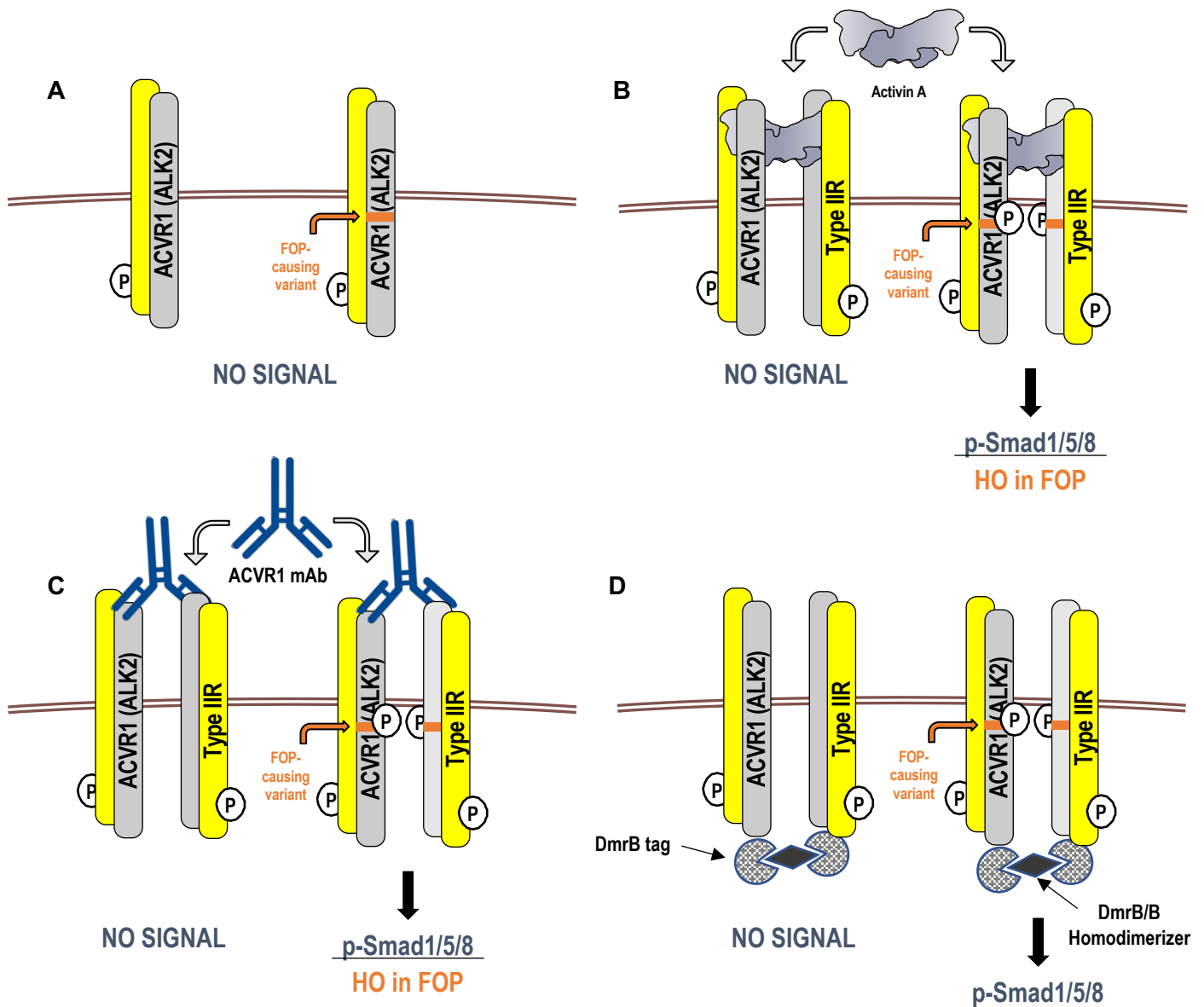
**Supplemental Figure 12: ACVR1 antibodies alter the progression and amount of heterotopic bone formed in FOP mice.**

Representative  $\mu$ CT images of FOP mice (*Acvr1*<sup>[R206H]FlEx/+</sup>; *GT(ROSA26)Sor*<sup>CreERT2/+</sup> post-tamoxifen) treated with ACVR1 mAb 1 or isotype control antibody. At 2 weeks post initiation of HO, ACVR1 mAb 1 treated animals appears less mature than those treated with isotype control. By 3 weeks after model initiation, the heterotopic bone lesions formed in ACVR1 mAb 1 treated mice have matured and are much larger than those lesions observed in isotype mAb control treated mice.



**Supplemental Figure 13: HO formed after ACVR1 antibody treatment shows the expected features of endochondral bone formation.**

H&E-stained sections of growing heterotopic bone lesions from mAb 1 (**A**) or mAb 3 (**B**) demonstrate fibroproliferation (arrows), chondrogenesis (arrowheads), and bone formation (#) with the development of bone marrow (\*) in the HO lesions.



**Supplemental Figure 14: ACVR1 antibodies act as an Activin A mimic on FOP-mutant ACVR1.**

(A) WT ACVR1 and FOP-causing variants of ACVR1 (grey) form ligand-independent heterodimers with the Type II receptors (yellow). (B) Activin A forms a non-signaling complex with WT ACVR1 and type II receptors. In contrast, a stoichiometrically identical complex wherein ACVR1 is FOP-mutant activates Smad1/5/8 phosphorylation and HO in FOP. (C) ACVR1 antibodies bring together ACVR1 and the associated type II receptors. Dimerization of FOP-causing variants of ACVR1 with antibodies activates Smad1/5/8 signaling and HO in FOP cells and mice, whereas antibody-mediated dimerization of WT ACVR1 in complex with type II receptors does not result in signaling. (D) Intracellular dimerization of DmrB-tagged FOP mutant ACVR1 using the DmrB/B homodimerizer activates Smad1/5/8 signaling, indicating that FOP-mutant ACVR1 is activated by dimerization irrespective of the manner by which it is induced. Dimerization of WT ACVR1 by the same means does not result in signaling.